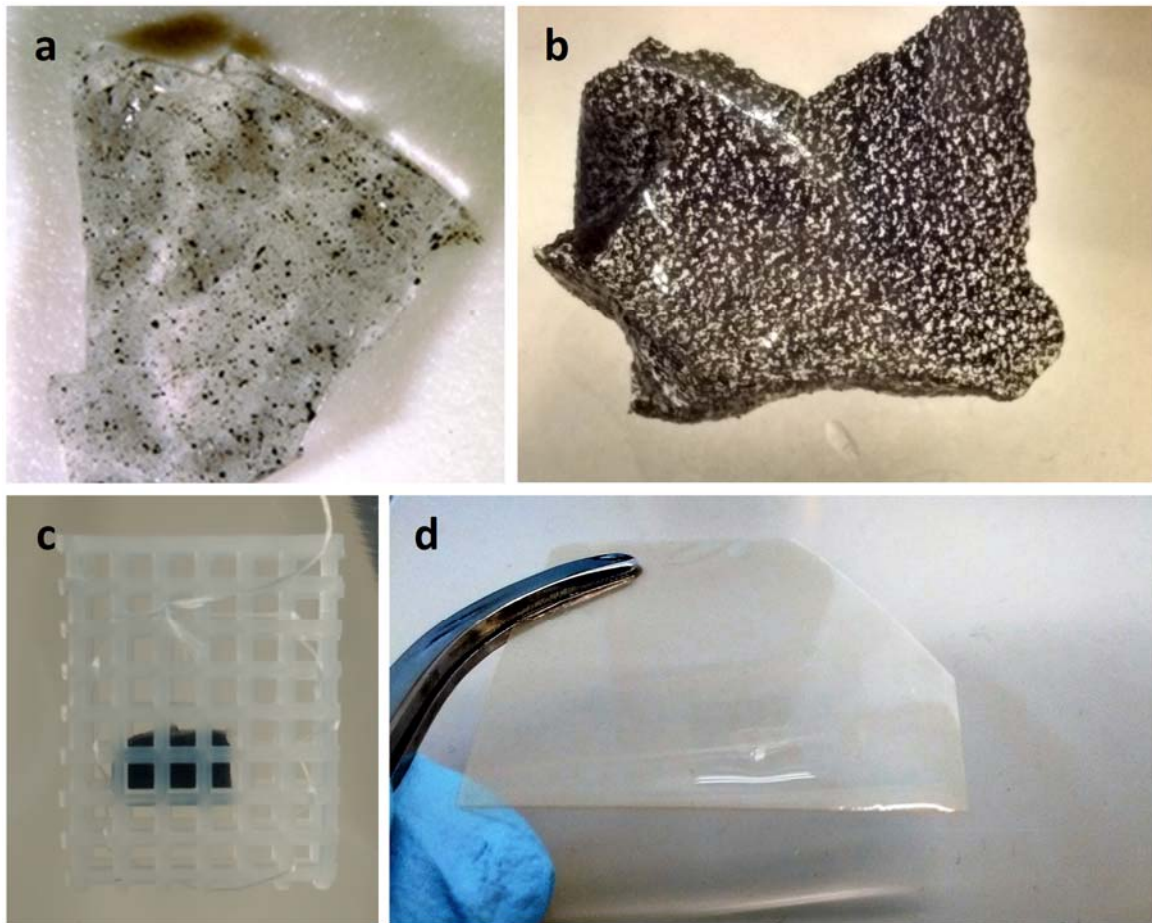


This work was written as part of one of the author's official duties as an Employee of the United States Government and is therefore a work of the United States Government. In accordance with 17 U.S.C. 105, no copyright protection is available for such works under U.S. Law. Access to this work was provided by the University of Maryland, Baltimore County (UMBC) ScholarWorks@UMBC digital repository on the Maryland Shared Open Access (MD-SOAR) platform.

Please provide feedback

Please support the ScholarWorks@UMBC repository by emailing scholarworks-group@umbc.edu and telling us what having access to this work means to you and why it's important to you. Thank you.



1
2 **Figure S1.** Photos of select sampling materials. (a) ag+AC under light microscope; (b)
3 PVDF+AC under light microscope; (c) ag+AC in protective basket; (d) PET+Cys.

4 **Table S1.** Raw data and calculations from sediment and soil slurry experiment at d 0.^a

Matrix	Rep	Sampler	Sulfide	pH	C_s	C_{pw}	$\log K_d$
			(μM)		(ng kgdw ⁻¹)	(ng L ⁻¹)	$\log (L \text{ kgdw}^{-1})$
sediment	1	n/a	0.69	7.06	945	0.5	3.31
sediment	2	n/a	0.69	6.98	1149	0.3	3.55
sediment	3	n/a	0.69	6.80	993	0.5	3.33
soil	1	n/a	267.00	7.04	74877	93.1	2.91
soil	2	n/a	270.92	7.07	45118	90.6	2.70
soil	3	n/a	268.95	7.04	44690	79.6	2.75

5 ^a C_s and C_{pw} are concentrations of MeHg in solids and porewater, respectively.

6 **Table S2.** Raw data and calculations from sediment and soil slurry experiment at d 20.^a

Matrix	Rep	Sampler	Sulfide	pH	C _s	C _{pw}	log K _d	C _{ps}	C _{pw} Pred. w. K _{SRHA}	Avg.	Std. Error	log K _{pw}
			(μ M)		(ng kgdw ⁻¹)	(ng L ⁻¹)	log (L kgdw ⁻¹)	(ng kg ⁻¹)	(ng L ⁻¹)	(ng L ⁻¹)	(ng L ⁻¹)	log (L kg ⁻¹)
sediment	1	ag+AC	0.09	6.88	554	0.58*	n.d.	58	0.09			n.d.
sediment	2	ag+AC	0.05	7.10	562	0.13	3.64	59	0.09	0.09	0.00	2.66
sediment	1	ag+SAMMS	0.07	7.24	518	0.19	3.44	116	0.11			2.79
sediment	2	ag+SAMMS	0.08	7.30	614	0.10	3.78	92	0.09	0.05	0.01	2.95
sediment	1	PET+Cys	0.07	7.25	587	0.09	3.83	289	0.44			3.52
sediment	2	PET+Cys	0.05	7.13	623	0.09	3.86	10	0.01	0.08	0.07	2.05
soil	1	ag+AC	0.54	7.14	44049	8.07	3.74	19433	30.10			3.38
soil	2	ag+AC	0.87	7.10	48468	7.96	3.78	22123	34.26	30.73	1.99	3.44
soil	1	ag+SAMMS	0.95	7.15	45573	7.17	3.80	12227	11.95			3.23
soil	2	ag+SAMMS	0.65	7.11	41233	11.30	3.56	10791	10.55	5.64	0.35	2.98
soil	1	PET+Cys	1.06	7.21	46701	9.41	3.70	11546	17.48			3.09
soil	2	PET+Cys	0.62	7.17	47668	8.14	3.77	10761	16.29	5.72	0.20	3.12

7 ^a All concentrations are of MeHg.8 * Excluded from calculations for failing *Q*-test.



9

10 **Figure S2.** Photos of sediment microcosm experiment. (a) Overview of setup; (b, c) detail views
11 of one beaker from the side and above. Note placement of baskets to expose passive samplers to
12 visibly apparent redox transition zone.

13 **Analytical Methods.** MeHg samples were distilled in H₂SO₄ as described by Horvat and others
14 (1993) and analyzed following the method outlined by Mitchell and Gilmour (2008). Briefly, a
15 spike consisting of enriched, stable Hg isotope (Oak Ridge National Laboratories) was added,
16 the samples were buffered with acetate, derivatized with sodium tetraethylborate to facilitate
17 volatilization, purged and concentrated on a Tenax trap with a BrooksRand autosampler,
18 thermally desorbed, separated on an OV-3/Chromosorb column, and introduced into a Perkin
19 Elmer Elan DRC II ICP-MS for detection. THg was also measured as in Mitchell and Gilmour
20 (2008). Concentrations were determined by digesting samples in 7:4 HNO₃:H₂SO₄, heating to
21 achieve loss of color, oxidizing organics with BrCl, reducing Hg(II) to Hg(0) with SnCl₂, and
22 analyzing via ICP-MS. Isotopic dilution calculations were performed to enhance the accuracy
23 and precision of MeHg and THg measurements (Mitchell and Gilmour 2008). MeHg quality
24 assurance data are summarized in Table S3. Sulfide was measured by mixing samples 1:1 with
25 sulfide antioxidant buffer (2.0 M NaOH, 0.2 M ascorbic acid, and 0.2 M Na₂EDTA in
26 deoxygenated, deionized water prepared anaerobically) and analyzing with a sulfide ion-
27 selective electrode calibrated by lead titration of a saturated sulfide standard. DOC was measured
28 on a Shimadzu organic carbon analyzer. Cations were measured on a Perkin Elmer Optima 8300
29 ICP-OES. Where not directly measured, major ion concentrations used in speciation modeling
30 were estimated from the chemical composition of Instant Ocean provided by the manufacturer
31 (Spectrum Brands 2008).

32 **Table S3.** Quality assurance data for MeHg analyses in this work.^a

Matrix	RPD Duplicates	CRM Recovery	ID Spike Recovery	Distillation Blanks	DL	Units
water	6.2 ± 2.4%	95.8 ± 1.9%	70.3 ± 1.1%	0.52 ± 0.28	1.02 ± 0.27	ng L ⁻¹
sediment/ soil	22.6 ± 0.7%	105.1 ± 4.2%	59.8 ± 3.8%	0.51 ± 0.13	66.3 ± 11.2	ng kgdw ⁻¹
ag+AC	n/a	97.3 ± 2.2%	54.8 ± 2.3%	0.06 ± 0.01	228.66 ± 52.53	ng kgww ⁻¹
PET+Cys	n/a	99.7 ± 4.4%	61.1% ± 3.4%	0.05 ± 0.01	188.63 ± 27.84	ng kgww ⁻¹

33 ^a Analysis was done by isotope dilution ICP-MS, i.e. with internal stable isotope standards.

34 Relative percent differences (RPD) are for duplicate analyses of the same prepared sample.

35 CRMs were NIST 1566b oyster tissue. Detection limits were estimated as three times the

36 standard error of blanks across samples.

37 **Table S4.** Additional reactions used in MINEQL+ equilibrium speciation modeling.

Reaction	log K	Reference
$\text{H}^+ + \text{DOMRS}^- \rightleftharpoons \text{DOMRSH}$	9.000	(Karlsson and Skyllberg 2003; Liem-Nguyen and others 2016)
$\text{MeHg}^+ + \text{SO}_4^{2-} \rightleftharpoons \text{MeHgSO}_4^-$	0.940	(Rabenstein and others 1976)
$\text{MeHg}^+ + \text{Br}^- \rightleftharpoons \text{MeHgBr}$	6.620	(Schwarzenbach and Schellenberg 1965)
$\text{MeHg}^+ + \text{Cl}^- \rightleftharpoons \text{MeHgCl}$	5.400	(Loux 2007)
$\text{MeHg}^+ + \text{F}^- \rightleftharpoons \text{MeHgF}$	1.500	(Schwarzenbach and Schellenberg 1965)
$\text{MeHg}^+ + \text{DOMRS}^- \rightleftharpoons \text{MeHgDOMRS}$	17.500	(Karlsson and Skyllberg 2003; Liem-Nguyen and others 2016; Qian and others 2002; Reid and Rabenstein 1981)
$2\text{MeHg}^+ + \text{H}_2\text{O} \rightleftharpoons (\text{MeHg})_2\text{OH}^+ + \text{H}^+$	-2.150	(De Robertis and others 1998)
$\text{MeHg}^+ + \text{H}_2\text{O} \rightleftharpoons \text{MeHgOH} + \text{H}^+$	-4.500	(Loux 2007)
$\text{MeHg}^+ + \text{CO}_3^{2-} + \text{MeHgCO}_3^-$	6.100	(Rabenstein and others 1976)
$\text{MeHg}^+ + \text{H}^+ + \text{CO}_3^{2-} \rightleftharpoons \text{MeHgHCO}_3$	12.950	(Loux 2007)
$\text{MeHg}^+ + \text{HS}^- \rightleftharpoons \text{MeHgS}^- + \text{H}^+$	7.300	(Schwarzenbach and Schellenberg 1965)
$\text{MeHg}^+ + \text{HS}^- \rightleftharpoons \text{MeHgSH}$	14.500	(Dyrssen and Wedborg 1991)



38 ^a Two components were added to the software's database: MeHg (+1 charge), and DOMRS,
39 representing a model reduced exocyclic sulfur binding site in Suwannee River Humic Acid (-1
40 charge). DOMRS site densities were estimated from DOC measurements with the following
41 equation, under the assumption that DOM characteristics were similar to SRHA (Graham and
42 others 2017; Manceau and Nagy 2012; IHSS 2017):

43

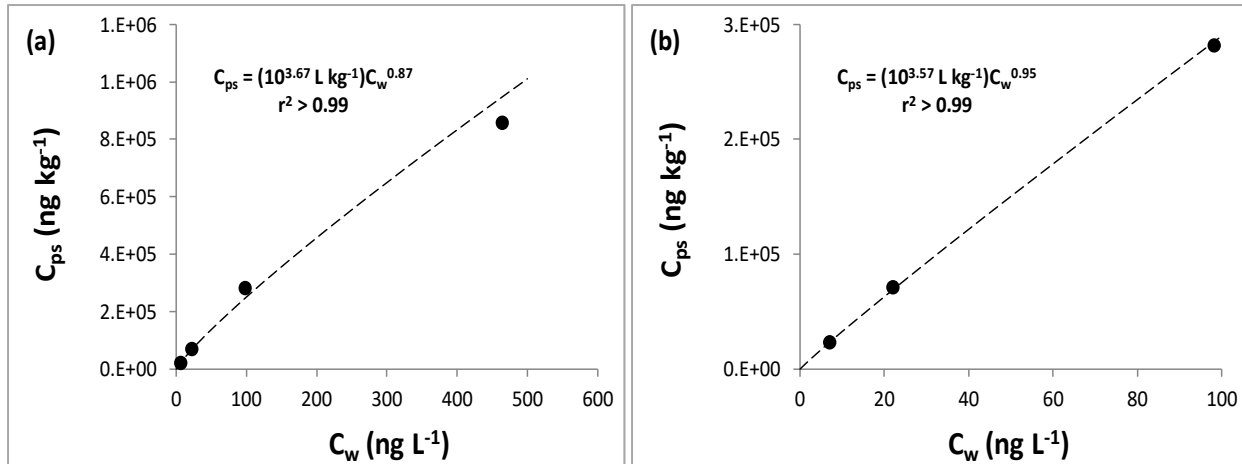
$$\text{[DOMRS]} = \frac{\text{mg DOC}}{\text{L}} \times \frac{\text{mg SRHA}}{0.5263 \text{ mg DOC}} \times \frac{0.0054 \text{ mg S}}{\text{mg SRHA}} \times \frac{0.236 \text{ mg reduced exocyclic S}}{\text{mg S}}$$

44

$$\times \frac{\text{mol reduced exocyclic S}}{32065 \text{ mg reduced exocyclic S}}$$

45

46



48 **Figure S3.** Freundlich model fits of sorption isotherm data for MeHgOH on ag+AC. Points:
49 measured data. Dashed lines: model fits (equations shown on plots). (a) All four points; (b) first
50 three points only.

51 **Sampling Mechanisms.** Using MeHg partitioning coefficients for bare AC (Gomez-Eyles and
52 others 2013) and Thiol-SAMMS (the present work), we conducted a simple, mass-weighted
53 partitioning analysis for the samplers containing suspensions of these sorbent materials, as
54 follows:

$$55 \quad K_{pw,predicted} = f_{polymer}K_{polymer} + f_{sorbent}K_{sorbent} \quad (S1)$$

56 where f is the fractional contribution of each component to the total mass of the material.
57 Because these calculations involved K values separated by multiple orders of magnitude, they
58 were accompanied by substantial uncertainty. Even so, a comparison of measured K_{pw} to
59 $K_{pw,predicted}$ provided a semiquantitative indication of the relative contributions of internal
60 diffusion and surface adsorption to the overall mechanisms of sampler accumulation (Table S5).
61 Notably, the agarose-based samplers performed more closely to model predictions than did the
62 PVDF-based samplers, indicating that the former were more permeable and amenable to
63 suffusion by MeHgOH. Indeed, MeHg species are known to pass readily through agarose, which

64 is sometimes used as the diffusive gel in DGT samplers (Fernández-Gómez and others 2014;
65 Gao and others 2014). A diffusive mechanism for ag+AC was confirmed in the subsequent
66 kinetics experiment.

67 In an attempt to enhance the permeability of PVDF samplers, variants were prepared with either
68 water or 1:1 methanol:water as nonsolvent to produce contrasting membrane pore structures
69 (Sukitpaneenit and Chung 2009). The measured partitioning by the methanol:water-prepared
70 sampler, which was formulated to encourage a more globular microstructure with fewer
71 macrovoids, was somewhat greater than that of the water-prepared sampler ($\log K_{pw} = 3.73$ vs.
72 3.16). However, both remained well below their model-predicted partitioning, likely due to the
73 dense outer skin that is characteristic of PVDF membranes regardless of the nonsolvent used in
74 preparation (Sukitpaneenit and Chung 2009). Thus, it appears likely that partitioning by all of the
75 PVDF samplers in this study was dominated by surface adsorption and that most of the included
76 sorbent particles were not accessed by MeHgOH. An analogous method to modulate the
77 permeability of agarose was also explored. Alternate versions of ag+AC and ag+SAMMS were
78 prepared with a polyethylene glycol dopant to promote macroporosity in the gel (agPEG+AC
79 and agPEG+SAMMS; Charlionet and others 1996). The effects of this modification on isotherm
80 partitioning were ambiguous. While their measured and predicted K_{pw} values were in better
81 agreement than those of ag+AC and ag+SAMMS, this was due to increased partitioning by
82 agPEG+AC on one hand and decreased partitioning by agPEG+SAMMS on the other; no overall
83 trend was apparent. Additionally, the agPEG gels themselves were slushier and less
84 mechanically robust than standard agarose, making them poorly suited for deployment in
85 sediment and soil, so the idea was abandoned.

Table S5. Freundlich fitting parameters for MeHg isotherm experiments^a

Abbreviation	Material	Target Sorbent Conc.	MeHgOH			MeHgSRHA		
			log K _{pw} ^b	p-value	1/n	log K _{pw} ^b	p-value	1/n
ag	agarose	n/a	3.18 ± 0.12	0.0014	0.54	n.d.	n.d.	n.d.
ag+AC	activated carbon suspended in agarose	10% w/w AC	3.67 ± 0.08	0.0005	0.86	2.91 ± 0.08	<0.0001	0.93
ag+Cys	L-cysteine dissolved in agarose	2% w/w Cys	2.84 ± 0.23	0.0011	1.04	n.d.	n.d.	n.d.
ag+Cys-alg	L-cysteine-functionalized alginate suspended in agarose	5% w/w Cys	4.12 ± 0.24	<0.0001	0.70	n.d.	n.d.	n.d.
ag+Cys-xylo	L-cysteine-functionalized xyloglucans suspended in agarose	5% w/w Cys	3.47 ± 0.24	0.0005	0.73	n.d.	n.d.	n.d.
ag+MAA-chit	mercapto-functionalized chitosan suspended in agarose	0.3% w/w mercapto	3.47 ± 0.19	0.0004	0.88	n.d.	n.d.	n.d.
ag+MPTMS-DE	mercapto-functionalized diatomaceous earth suspended in agarose	1% w/w mercapto	4.23 ± 0.09	<0.0001	0.73	3.29 ± 0.07	<0.0001	0.82
ag+SAMMS	thiol-SAMMS suspended in agarose	2% w/w SAMMS	4.95 ± 0.16	<0.0001	1.03	3.50 ± 0.15	0.00	0.76
agPEG	agarose doped with polyethylene glycol and glycerol	n/a	3.28 ± 0.23	0.00007	0.46	n.d.	n.d.	n.d.

agPEG+AC	activated carbon suspended in PEG-doped agarose	3% w/w AC	4.11 ± 0.15	0.0001	0.72	3.21 ± 0.20	0.0005	0.78
agPEG+SAMMS	thiol-SAMMS suspended in PEG-doped agarose	2% w/w SAMMS	4.01 ± 0.04	<0.0001	0.96	2.81 ± 0.06	<0.0001	1.14
CA	cellulose acetate	n/a	2.95 ± 0.07	<0.0001	0.63	n.d.	n.d.	n.d.
CA+MA	mercapto-functionalized cellulose acetate	20% w/w mercapto	2.21 ± 0.19	0.0075	1.06	n.d.	n.d.	n.d.
CN	cellulose nitrate	n/a	3.22 ± 0.18	0.0004	0.69	n.d.	n.d.	n.d.
DE	diatomaceous earth	n/a	3.16 ± 0.13	<0.0001	0.69	n.d.	n.d.	n.d.
MPTMS-DE	mercapto-functionalized diatomaceous earth	3% w/w mercapto	5.52 ± 0.07	<0.0001	1.24	n.d.	n.d.	n.d.
Parafilm	paraffin	n/a	1.93 ± 0.20	0.0023	1.07	n.d.	n.d.	n.d.
PDMS	polydimethylsiloxane	n/a	2.56 ± 0.04	0.0006	0.57	n.d.	n.d.	n.d.
PES	polyethersulfone	n/a	2.78 ± 0.38	0.0052	0.76	n.d.	n.d.	n.d.
PET+Cys	L-cysteine-functionalized polyethylene terephthalate	8 nmol Cys cm ⁻²	4.39 ± 0.21	0.0002	0.62	3.61 ± 0.07	<0.0001	0.55

POM38	polyoxymethylene (38 μm thick)	n/a	2.58 ± 0.13	0.0003	0.54	n.d.	n.d.	n.d.
PTFE	polytetrafluoroethylene	n/a	2.58 ± 0.11	0.0002	0.67	n.d.	n.d.	n.d.
PVDFm+AC	activated carbon suspended in PVDF prepared with 1:1 methanol:water nonsolvent	10% w/w AC	3.74 ± 0.32	0.007	0.89	n.d.	n.d.	n.d.
PVDFw	polyvinylidene fluoride prepared with water nonsolvent	n/a	2.77 ± 0.29	0.0102	0.68	n.d.	n.d.	n.d.
PVDFw+AC	activated carbon suspended in PVDF prepared with water nonsolvent	10% w/w AC	3.39 ± 0.20	0.0036	0.92	3.51 ± 0.02	<0.0001	0.62
PVDFw+Cys	L-cysteine dissolved in PVDF	6% w/w Cys	5.27 ± 0.11	<0.0001	0.55	n.d.	n.d.	n.d.
PVDFw+SAMMS	thiol-SAMMS suspended in PVDF	5% w/w SAMMS	4.41 ± 0.15	<0.0001	0.82	2.85 ± 0.10	0.0001	1.12
SAMMS	thiol-SAMMS	n/a	n.d.	n.d.	n.d.	5.17 ± 0.16	<0.0001	n.d.

^a Experimental data fit to a Freundlich adsorption isotherm model.

^b Partition coefficient $\pm 1\text{SE}$

86 References or sources for polymers and sorbents: ag: Gao and others 2011; Cys+alg: Bernkop-Schnürch and others 2001; Cys+xylo:
87 Bhalekar and others 2013; ag+MAA-chit: Kast and Bernkop-Schnürch 2001; ag+MPTMS-DE: Yu and others 2012; SAMMS:
88 Steward Environmental Solutions; agPEG: Charlionet and others 1996; CA: Membrane Filtration Products Inc.; MA: Aoki and others
89 2007; CN: Membrane Filtration Products Inc.; DE: Honeywell, Muskegon, MI; MPTMS-DE: Yu and others 2012; parafilm: Bemis,
90 Oshkosh, WI; PDMS: Altec, St. Austell, UK; PES: Goodfellow Cambridge, Inc. Huntington, UK; PET+Cys: Duan and Lewis 2002;
91 POM38: CS Hyde, Lake Villa, IL; PTFE: Grainger, Lake Forest, IL.

92 **Table S6.** Comparison of measured sampler partitioning in isotherm studies ($\log K_{pw}$) to mass-weighted predictions based on
 93 fractional compositions of polymer ($f_{polymer}$) and sorbent ($f_{sorbent}$).

Abbreviation	Material	$\log K_{pw}$	p	$f_{polymer}$	$f_{sorbent}$	$\log K_{pw,predicted}$	Ratio $K_{pw} : K_{pw,predicted}$
ag	agarose	2.06	0.0018	n/a	n/a	n/a	n/a
agPEG	agarose doped with polyethylene glycol and glycerol	2.17	0.0367	n/a	n/a	n/a	n/a
PVDFw	poly(vinylidene fluoride) prepared with water nonsolvent	2.11	0.0009	n/a	n/a	n/a	n/a
AC	activated carbon	5.22	0.0004	n/a	n/a	n/a	n/a
ag+AC	activated carbon suspended in agarose	3.46	0.0004	0.96	0.04	3.8	0.43
agPEG+AC	activated carbon suspended in PEG-doped agarose	3.28	0.0001	0.97	0.03	3.4	0.76
PVDFw+AC	AC suspended in PVDF prepared with water nonsolvent	3.16	0.0003	0.89	0.11	3.9	0.17
PVDFm+AC	AC suspended in PVDF prepared with 1:1 methanol:water nonsolvent	3.73	0.0003	0.89	0.11	4.3	0.29

94 ^a See text above for prediction equation.

95 **Table S7.** Raw data and calculations for initial passive sampler kinetics experiment.

Sorbate	Sampler	t (min)	C _w (ng L ⁻¹)	C _{ps} (ng kg ⁻¹)	ng on ps	ng in Water	Mass Bal.	% Recov.	C _{ps:C_w}	log (C _{ps:C_w})	Frac. Equil. vs. Isotherm
MeHgOH	ag+AC	1411	1.75	666	0.018	0.087	0.106	46%	381	2.58	0.14
MeHgOH	ag+AC	10029	0.16	2210	0.021	0.008	0.028	12%	13984	4.15	4.96
MeHgOH	ag+AC	20077	0.10	1042	0.017	0.005	0.021	9%	10582	4.02	3.75
MeHgOH	ag+AC	40250	0.03	1799	0.010	0.002	0.012	5%	56340	4.75	19.99
MeHgOH	PET+Cys	1390	3.13	977	0.017	0.159	0.176	76%	312	2.49	0.06
MeHgOH	PET+Cys	10008	0.12	1184	0.021	0.006	0.026	11%	9937	4.00	1.85
MeHgOH	PET+Cys	20056	0.06	1559	0.025	0.003	0.028	12%	25002	4.40	4.66
MeHgOH	PET+Cys	40231	0.09	1281	0.017	0.004	0.021	9%	14575	4.16	2.71
MeHgSRHA	ag+AC	433	11.22	806	0.010	0.566	0.576	58%	72	1.86	0.11
MeHgSRHA	ag+AC	1405	6.42	287	0.007	0.330	0.337	34%	45	1.65	0.07
MeHgSRHA	ag+AC	10018	12.56	1370	0.024	0.634	0.657	66%	109	2.04	0.16
MeHgSRHA	ag+AC	20067	8.69	813	0.016	0.442	0.458	46%	93	1.97	0.14
MeHgSRHA	ag+AC	40240	3.43	2049	0.034	0.175	0.209	21%	597	2.78	0.88
MeHgSRHA	ag+AC	79404	0.85	554	0.012	0.043	0.055	5%	651	2.81	0.96
MeHgSRHA	PET+Cys	429	11.30	2155	0.048	0.569	0.617	62%	191	2.28	0.10

MeHgSRHA	PET+Cys	1389	15.00	899	0.020	0.767	0.787	79%	60	1.78	0.03
MeHgSRHA	PET+Cys	10001	2.57	400	0.009	0.129	0.138	14%	155	2.19	0.08
MeHgSRHA	PET+Cys	20050	6.40	1441	0.019	0.328	0.347	35%	225	2.35	0.12
MeHgSRHA	PET+Cys	40223	2.14	825	0.017	0.104	0.121	12%	386	2.59	0.20
MeHgSRHA	PET+Cys	79388	0.48	1997	0.022	0.024	0.047	5%	4139	3.62	2.12

⁹⁶ ^a All concentrations are of MeHg. Mass balances in samples showed loss of MeHg over time, especially in isotherms without added
 97 SRHA. This resulted in artificially reduced C_w at later time points and partitioning that surpassed the 14-d K_{pw} values generated in
 98 screening isotherms. Mass balances in MeHgSRHA samples were somewhat more favorable, indicating a preservative effect of either
 99 SRHA or the accompanying buffer.

Table S8. Mass balance data for ag+AC thick/thin sampler kinetics experiment.

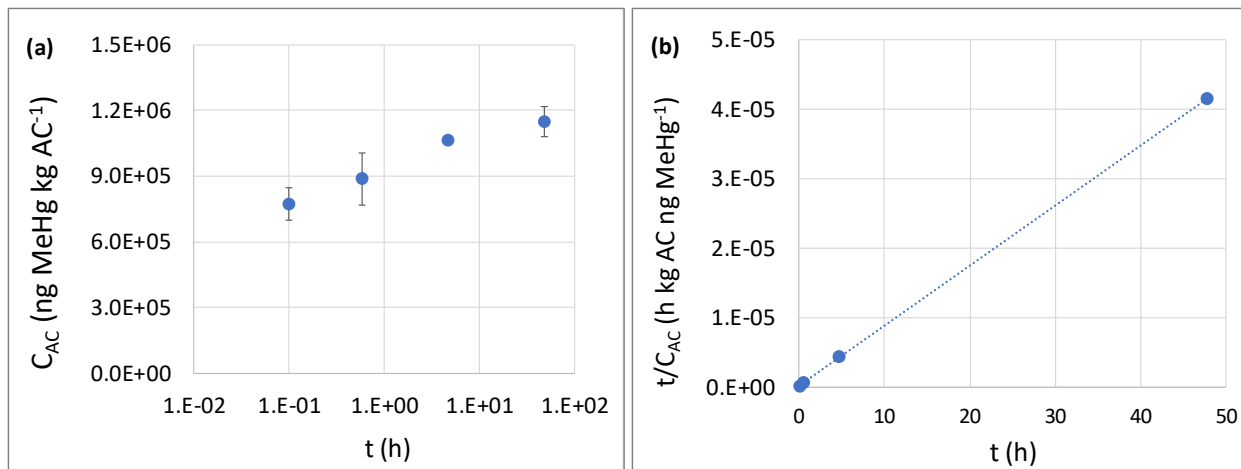
Time Pt.	ag+AC	g Water	Final C _w (ng L ⁻¹)	ng in Water	ng in Sampler	Total ng	Frac. Recov.
0	none	37.437	45.77	1.713	0.000	1.713	92%
0	thick	40.317	48.76	1.966	0.018	1.984	98%
0	thin	39.320	49.78	1.957	0.022	1.979	101%
1	none	36.519	48.25	1.762	0.000	1.762	97%
1	thick	38.434	47.71	1.834	0.028	1.862	97%
1	thin	37.636	48.59	1.829	0.040	1.869	99%
1	none	39.413	48.92	1.928	0.000	1.928	98%
1	thick	39.840	45.99	1.832	0.028	1.860	93%
1	thin	37.262	46.44	1.730	0.037	1.767	95%
2	none	35.790	51.99	1.861	0.000	1.861	104%
2	thick	38.035	50.68	1.928	0.031	1.958	103%
2	thin	39.596	50.66	2.006	0.050	2.056	104%
3	none	37.717	48.47	1.828	0.000	1.828	97%
3	thick	39.623	49.97	1.980	0.066	2.046	103%
3	thin	38.236	47.71	1.824	0.096	1.920	100%
4	none	36.918	49.62	1.832	0.000	1.832	99%
4	thick	38.405	51.84	1.991	0.165	2.156	112%
4	thin	39.172	50.90	1.994	0.222	2.216	113%
5	none	39.288	48.11	1.890	0.000	1.890	96%
5	thick	39.138	42.42	1.660	0.240	1.900	97%
5	thin	39.306	49.67	1.952	0.432	2.384	121%
5	none	39.027	51.73	2.019	0.000	2.019	103%
5	thick	40.596	52.98	2.151	0.237	2.388	118%
5	thin	39.471	44.78	1.768	0.293	2.060	104%

6	none	37.938	45.68	1.733	0.000	1.733	91%
6	thick	40.371	39.30	1.586	0.518	2.104	104%
6	thin	39.435	36.16	1.426	0.607	2.033	103%
7	none	40.326	49.90	2.012	0.000	2.012	100%
7	thick	38.901	32.21	1.253	0.297	1.550	80%
7	thin	38.012	33.87	1.288	0.308	1.596	84%

101 ^a All concentrations are of MeHg. All samples were spiked to an initial concentration of 50 ng L⁻¹
 102 ¹. Average fractional recovery was 102 ± 7% (s.d. among all 30 samples).

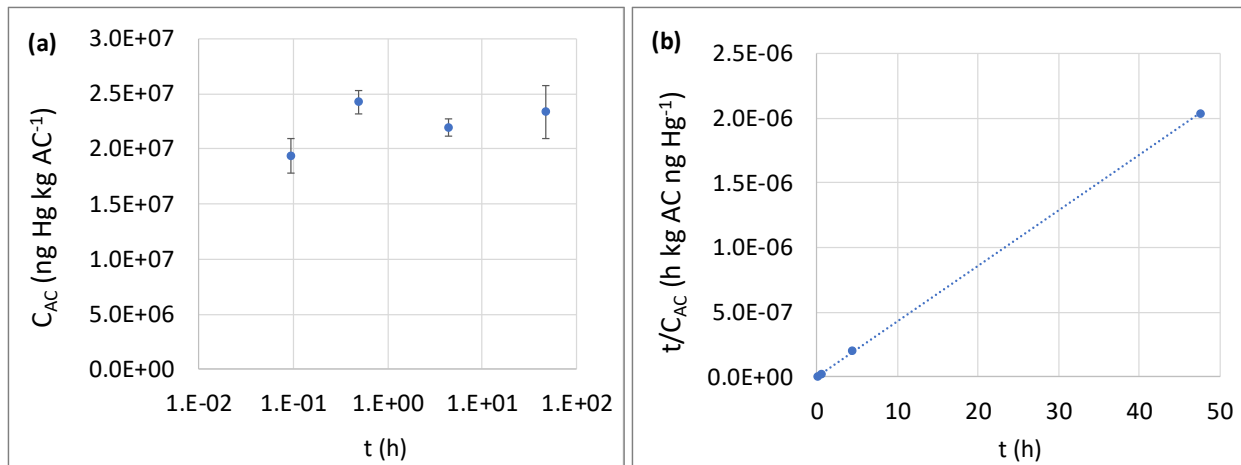
103 **Activated Carbon Kinetics Modeling.** The MeHg-AC kinetic data (Figure S4a) were fitted
 104 with pseudo-first order (Lagergren 1898) and pseudo-second order (Ho and McKay 1998)
 105 (Figure S4b) kinetic models. Both models provided good fits of the data ($r^2 = 0.98$ and 1.0,
 106 respectively), suggesting a Langmuir-type adsorption mechanism (Tien and Ramarao 2017). The
 107 apparent sorption rate constants, which depend on experimental conditions including initial C_w,
 108 were $k_1 = 0.31 \text{ h}^{-1}$ and $k_2 = 2.1 \times 10^{-4} \text{ kg ng}^{-1} \text{ h}^{-1}$. The equilibrium C_{AC} predicted by the pseudo-
 109 second order model was $1.2 \times 10^6 \text{ ng kg}^{-1}$. It should be emphasized that this does not represent
 110 this AC's maximum adsorptive capacity. In Gomez-Eyles et al., the MeHg sorption isotherm of
 111 this carbon remained log-linear for initial C_w values up to 6000 ng L⁻¹ under conditions nearly
 112 identical to ours. There, the final C_{AC} was $2.8 \times 10^7 \text{ ng kg}^{-1}$ (Gomez-Eyles and others 2013).
 113 This, along with the proportionality of our screening isotherms, indicates that there is little
 114 danger of saturating an ag+AC sampler with MeHg at environmentally realistic C_{pw}. We also
 115 evaluated the kinetics of inorganic mercury sorption to AC (Table S9 and Figure S5).
 116

117



118 **Figure S4.** Kinetics of MeHgOH adsorption to a coal-derived activated carbon (initial $C_w = 250$
119 ng L⁻¹). (a) MeHg concentrations on AC over time; error bars show ± 1 standard error. (b)
120 Pseudo-second order model fit. $k_2 = 2.1 \times 10^{-4}$ kg ng⁻¹ h⁻¹; $C_{AC,eq} = 1.2 \times 10^6$ ng kg⁻¹.

121



122

123 **Figure S5.** Kinetics of Hg(OH)₂ adsorption to a coal-derived activated carbon (initial $C_w = 5000$
124 ng L⁻¹). (a) Hg concentrations on AC over time; error bars show ± 1 standard error. (b) Pseudo-
125 second order model fit. $k_2 = 1.1 \times 10^{-5}$ kg ng⁻¹ h⁻¹; $C_{AC,eq} = 2.3 \times 10^7$ ng kg⁻¹.

126

127

Table S9. Raw data and calculations for SRHA gradient experiment.

Sorbent	SRHA (mg L ⁻¹)	C _w (ng L ⁻¹)	m _w MeHg (ng)	m _{sorbent} MeHg (ng)	m sorbent (mg)	C _{sorbent} (ng g ⁻¹)	log K _d	Treatment Average log K _d
CAC-Coal	5	0.15	2.94	9.33	12	777.83	3.72	
CAC-Coal	5	0.14	2.75	9.52	10	952.17	3.84	3.77
CAC-Coal	5	0.15	2.95	9.32	11	847.00	3.76	
CAC-Coal	25	0.22	4.32	5.68	10	557.28	3.41	
CAC-Coal	25	0.29	5.76	4.24	10	423.64	3.17	3.29
CAC-Coal	25	0.23	4.56	5.44	13	431.81	3.28	
CAC-Coal	50	0.22	4.37	7.90	12	657.99	3.48	
CAC-Coal	50	0.33	6.62	5.65	10	565.35	3.23	3.35
CAC-Coal	50	0.26	5.24	7.03	12	586.23	3.35	
CAC-Coal	500	0.52	10.37	1.90	11	172.92	2.52	
CAC-Coal	500	0.30	6.03	6.24	12	520.02	3.24	2.86
CAC-Coal	500	0.45	9.00	3.27	11	297.19	2.82	
thiol-SAMMS	5	0.04	0.83	9.17	11	833.75	4.30	
thiol-SAMMS	5	0.04	0.72	9.28	12	773.14	4.33	4.30
thiol-SAMMS	5	0.04	0.89	9.11	11	827.83	4.27	
thiol-SAMMS	50	0.05	1.00	9.00	10	900.16	4.26	
thiol-SAMMS	50	0.05	0.97	9.03	10	903.28	4.27	4.26
thiol-SAMMS	50	0.05	0.98	9.02	10	902.37	4.27	
thiol-SAMMS	500	0.23	5.53	6.74	12	561.45	3.38	
thiol-SAMMS	500	0.07	1.78	10.49	11	873.80	4.07	3.84
thiol-SAMMS	500	0.08	1.89	10.38	10	943.53	4.07	

128

129

Table S10. Raw data and calculations for MeHg AC kinetics and desorption experiment.

Sorbent	Time Pt.	Rep	t (h)	C _w (ng L ⁻¹)	m _{tot} (ng)	m in Water (ng)	Frac. as Carry-over	ng on AC	mg AC	C _{AC} (ng kg ⁻¹)	C _{AC} :C _w (L kg ⁻¹)	Avg. log K
none	a1	1	0.08	6.60	0.976	0.32	n/a	n/a	n/a	n/a	n/a	n/a
none	a1	2	0.08	10.44	0.989	0.52	n/a	n/a	n/a	n/a	n/a	n/a
CAC-Coal	a1	1	0.10	90.81	11.762	4.27	n/a	7.490	10.70	699961	7708	
CAC-Coal	a1	2	0.10	61.80	13.103	3.24	n/a	9.864	11.61	849629	13749	4.03
none	a2	1	0.60	8.42	0.986	0.41	n/a	n/a	n/a	n/a	n/a	n/a
none	a2	2	0.60	9.84	1.037	0.51	n/a	n/a	n/a	n/a	n/a	n/a
CAC-Coal	a2	1	0.57	33.52	12.505	1.68	n/a	10.828	10.75	1007266	30054	
CAC-Coal	a2	2	0.58	69.52	12.658	3.52	n/a	9.138	11.89	768530	11055	4.31
none	a3	1	4.60	7.74	0.982	0.38	n/a	n/a	n/a	n/a	n/a	n/a
none	a3	2	4.62	9.94	1.013	0.50	n/a	n/a	n/a	n/a	n/a	n/a
CAC-Coal	a3	1	4.67	17.57	12.916	0.91	n/a	12.008	10.90	1101662	62691	
CAC-Coal	a3	2	4.67	19.64	12.732	1.00	n/a	11.732	11.33	1035469	52715	
CAC-Coal	a3	3	4.68	21.98	12.606	1.11	n/a	11.498	10.84	1060663	48262	4.74
none	a4	1	47.63	10.12	0.987	0.50	n/a	n/a	n/a	n/a	n/a	n/a
none	a4	2	47.65	10.05	1.009	0.51	n/a	n/a	n/a	n/a	n/a	n/a

CAC-Coal	a4	1	47.67	7.42	12.670	0.38	n/a	12.294	10.31	1192438	160639
CAC-Coal	a4	2	47.68	9.97	12.872	0.51	n/a	12.359	9.95	1242066	124554
CAC-Coal	a4	3	47.68	9.88	12.378	0.49	n/a	11.888	11.74	1012640	102455 5.11
none	d1	1	0.08	0.22	0.657	0.01	0.27	n/a	n/a	n/a	n/a
none	d1	2	0.08	0.23	0.476	0.01	0.34	n/a	n/a	n/a	n/a
CAC-Coal	d1	1	0.08	3.73	7.694	0.19	1.10	7.509	10.70	701737	188322
CAC-Coal	d1	2	0.10	5.77	10.044	0.29	0.61	9.749	11.61	839700	145601 5.27
none	d2	1	0.57	0.23	0.574	0.01	0.25	n/a	n/a	n/a	n/a
none	d2	2	0.57	0.26	0.531	0.01	0.32	n/a	n/a	n/a	n/a
CAC-Coal	d2	1	0.53	3.37	10.878	0.17	0.29	10.710	10.75	996271	295649
CAC-Coal	d2	2	0.53	8.86	9.259	0.46	0.26	8.796	11.89	739792	83479 5.28
none	d3	1	3.58	0.29	0.606	0.01	0.26	n/a	n/a	n/a	n/a
none	d3	2	3.60	0.30	0.513	0.01	0.23	n/a	n/a	n/a	n/a
CAC-Coal	d3	1	3.58	6.49	12.043	0.31	0.11	11.731	10.90	1076277	165899
CAC-Coal	d3	2	3.60	10.06	11.777	0.49	0.09	11.284	11.33	995906	98970
CAC-Coal	d3	3	3.60	10.08	11.536	0.50	0.08	11.041	10.84	1018515	101051 5.09
none	d4	1	43.28	0.24	0.493	0.01	0.43	n/a	n/a	n/a	n/a
none	d4	2	43.28	0.27	0.505	0.01	0.26	n/a	n/a	n/a	n/a
CAC-Coal	d4	1	43.30	1.62	12.312	0.08	0.22	12.231	10.31	1186325	733212

CAC-Coal	d4	2	43.32	1.96	12.376	0.10	0.18	12.278	9.95	1233927	630749	
CAC-Coal	d4	3	43.33	1.26	11.906	0.07	0.25	11.835	11.74	1008112	798736	5.86

131 ^a All concentrations are of MeHg.

132

Table S11. Raw data and calculations for Hg_i AC kinetics and desorption experiment.

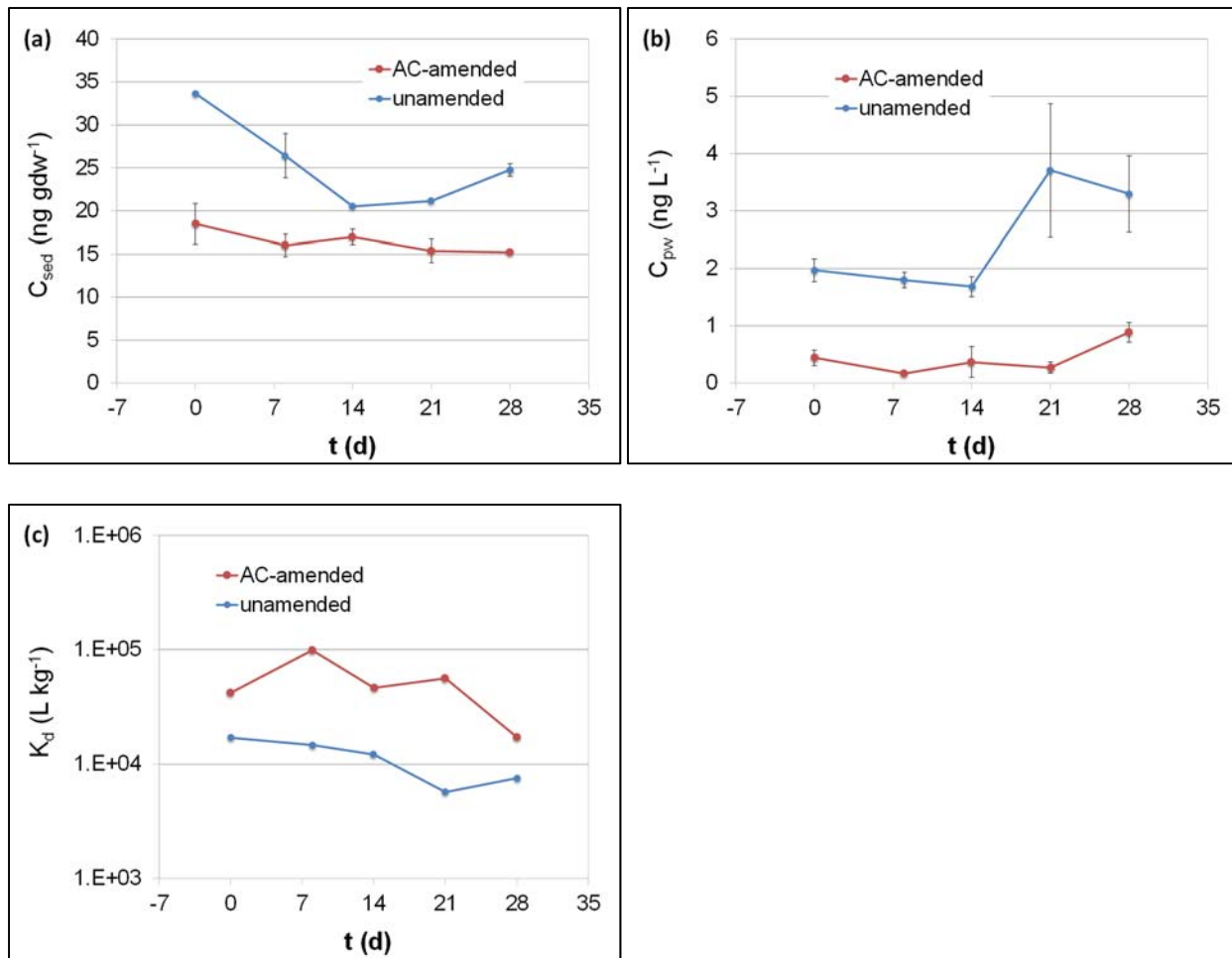
Sorbent	Time Pt.	Rep	t (h)	C _w (ng L ⁻¹)	m _{tot} (ng)	m in Water (ng)	Frac. as Carry-over	ng on AC	mg AC	C _{AC} (ng kg ⁻¹)	C _{AC} :C _w (L kg ⁻¹)	Avg. log K
none	a1	1	0.08	11.50	2.411	0.55	n/a	1.857	n/a	n/a	n/a	
none	a1	2	0.08	16.79	2.578	0.87	n/a	1.713	n/a	n/a	n/a	
CAC-Coal	a1	1	0.08	275.81	249.045	13.74	n/a	235.307	10.85	21687300	78631	
CAC-Coal	a1	2	0.12	123.07	244.370	6.01	n/a	238.355	11.90	20029845	162754	
CAC-Coal	a1	3	0.08	46.75	255.985	2.39	n/a	253.591	15.53	16329124	349250	5.29
none	a2	1	0.52	7.00	2.465	0.35	n/a	2.119	n/a	n/a	n/a	
none	a2	2	0.52	7.24	2.536	0.37	n/a	2.169	n/a	n/a	n/a	
CAC-Coal	a2	1	0.48	5.43	249.790	0.27	n/a	249.519	10.78	23146463	4264877	
CAC-Coal	a2	2	0.48	3.94	242.045	0.19	n/a	241.854	10.47	23099726	5858536	
CAC-Coal	a2	3	0.50	6.07	250.410	0.30	n/a	250.106	9.46	26438249	4353121	6.68
none	a3	1	4.32	11.63	2.497	0.58	n/a	1.916	n/a	n/a	n/a	
none	a3	2	4.32	19.26	2.523	0.97	n/a	1.552	n/a	n/a	n/a	
CAC-Coal	a3	1	4.33	9.51	255.325	0.49	n/a	254.839	11.28	22592138	2375327	
CAC-Coal	a3	2	4.35	11.97	249.750	0.60	n/a	249.152	12.24	20355561	1700461	
CAC-Coal	a3	3	4.38	16.34	249.340	0.82	n/a	248.525	10.89	22821393	1396340	6.26

none	a4	1	47.57	4.68	2.432	0.23	n/a	2.204	n/a	n/a	n/a
none	a4	2	47.58	15.43	2.554	0.79	n/a	1.766	n/a	n/a	n/a
CAC-Coal	a4	1	47.57	1.71	246.040	0.08	n/a	245.956	13.23	18590770	10876228
CAC-Coal	a4	2	47.57	1.36	247.125	0.07	n/a	247.058	9.36	26395060	19401360
CAC-Coal	a4	3	47.60	8.40	255.055	0.43	n/a	254.626	10.16	25061642	2981984
none	d1	1	0.08	1.18	1.861	0.06	0.07	n/a	n/a	n/a	n/a
none	d1	2	0.10	0.89	1.719	0.05	0.13	n/a	n/a	n/a	n/a
CAC-Coal	d1	1	0.08	10.72	236.095	0.57	1.38	235.526	10.85	21707439	2024606
CAC-Coal	d1	2	0.10	10.76	238.690	0.60	0.55	238.086	11.90	20007199	1859099
CAC-Coal	d1	3	0.10	29.23	253.730	1.57	0.09	252.155	15.53	16236656	555568
CAC-Coal	d2	1	0.58	17.11	249.526	0.85	0.01	248.676	10.78	23068300	1347896
CAC-Coal	d2	3	0.60	6.12	250.116	0.29	0.04	249.828	9.46	26408852	4316890
none	d3	1	3.78	0.59	1.920	0.03	0.06	n/a	n/a	n/a	n/a
none	d3	2	3.82	0.69	1.559	0.03	0.04	n/a	n/a	n/a	n/a
CAC-Coal	d3	1	3.82	8.19	254.864	0.45	0.03	254.413	11.28	22554311	2754905
CAC-Coal	d3	2	3.83	8.01	249.185	0.40	0.08	248.781	12.24	20325208	2538295
CAC-Coal	d3	3	3.82	14.17	248.582	0.73	0.09	247.853	10.89	22759688	1606712
none	d4	1	43.22	0.73	2.206	0.04	0.12	n/a	n/a	n/a	n/a
none	d4	2	43.23	0.97	1.773	0.05	0.11	n/a	n/a	n/a	n/a

CAC-Coal	d4	2	43.28	0.56	247.061	0.03	1.24	247.034	9.36	26392487	47329082
CAC-Coal	d4	3	43.30	0.66	254.640	0.04	0.19	254.600	10.16	25059095	38016674

134 ^a All concentrations are of Hg.

135



136

137 **Figure S6.** MeHg concentrations in (a) sediment and (b) porewater (directly measured); (c)
138 sediment-water partitioning in microcosm experiment. Error bars show ± 1 standard deviation (n
139 = 2).

Table S12. Porewater chemistry in unamended sediment used in microcosm experiment.

Parameter	Units	0 d	8 d	14 d	21 d	28 d
Al	mg L ⁻¹	2.06 ± 0.65	1.7 ± 0.57	1.31	1.03 ± 0.57	0.55 ± 0.4
B	mg L ⁻¹	0.98 ± 0.04	1 ± 0.12	1.1	1.13 ± 0.04	1.37 ± 0.16
Ba	mg L ⁻¹	1.15 ± 0.02	0.83 ± 0.25	0.79	1 ± 0.14	0.85 ± 0.46
Ca	mg L ⁻¹	81 ± 7	89 ± 18	111	125 ± 19	152 ± 16
DOC	mg L ⁻¹	n.d.	19.09 ± 1.92	17.02 ± 1.74	15.18 ± 1.01	35.91 ± 33.2
Fe	mg L ⁻¹	2.11 ± 0.34	3.44 ± 2.13	8.5	10.45 ± 8.7	14.08 ± 9.22
FMeHg	ng L ⁻¹	1.97 ± 0.19	1.8 ± 0.14	1.68 ± 0.17	3.71 ± 1.16	3.29 ± 0.67
FTHg	ng L ⁻¹	473.65 ± 145.59	414.37 ± 0.61	367.82	244.75 ± 59.89	143.69 ± 86.71
K	mg L ⁻¹	62.03 ± 7.83	54.1 ± 2.83	78.9	60.1 ± 9.48	91.05 ± 1.06
Mg	mg L ⁻¹	157 ± 7	167 ± 17	185	195 ± 22	254 ± 41
Mn	mg L ⁻¹	0.8 ± 0.1	0.92 ± 0.37	1.3	1.51 ± 0.65	2 ± 0.77
Na	mg L ⁻¹	1427 ± 21	1460 ± 14	1440	1495 ± 7	1935 ± 205
P	mg L ⁻¹	4.84 ± 0.18	5.94 ± 1.21	4.97	5.66 ± 0.64	5.61 ± 1.05
pH		6.95 ± 0.01	7.01 ± 0.47	6.54 ± 0.02	6.53 ± 0.18	6.45 ± 0.24
S	mg L ⁻¹	43.07 ± 10.29	55.85 ± 18.88	77.2	97.2 ± 37.9	138.15 ± 54.94
Si	mg L ⁻¹	15.33 ± 0.21	16.9 ± 0.42	16.9	15.4 ± 0.57	16.65 ± 0.78
Sr	mg L ⁻¹	1.22 ± 0.09	1.29 ± 0.21	1.56	1.7 ± 0.22	2.15 ± 0.3

sulfide	μM	0.44	0.82	1.42 ± 0.08	2.52 ± 0.35	1.32 ± 0.43
Zn	mg L^{-1}	0.32 ± 0.02	0.3 ± 0.05	0.35	0.34 ± 0.03	0.36 ± 0.01
MeHg (solid)	ng gdw^{-1}	33.64 ± 0.07	26.41 ± 2.56	20.52	21.13 ± 0.12	24.75 ± 0.76
THg (solid)	$\mu\text{g gdw}^{-1}$	45.71 ± 0.59	48.22 ± 0.58	46.78 ± 0.54	47.89 ± 1.56	49.25 ± 1.26

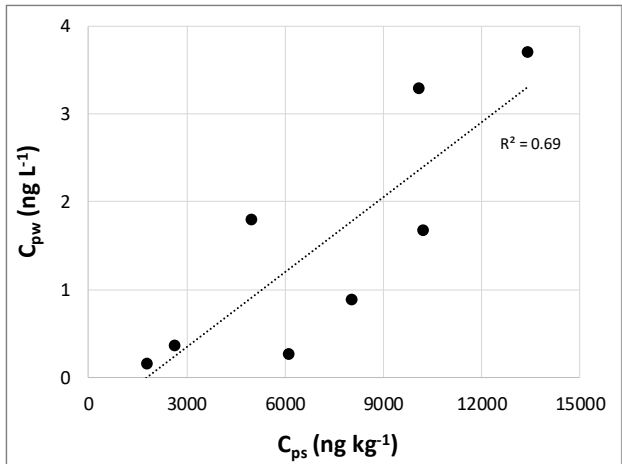
141 ^a Final two rows are solid-phase concentrations. Sediment was a silty mud collected to a depth of 15 cm from a tidal creek in the
 142 upper part of Berry's Creek in Bergen County, NJ. Values represent averages \pm one s.d. (no s.d. denotes $n = 1$).

Table S13. Porewater chemistry in AC-amended sediment used in microcosm experiment.

Parameter	Units	0 d	8 d	14 d	21 d	28 d
Al	mg L ⁻¹	0.79 ± 0.3	0.2 ± 0.1	0.57 ± 0.08	0.13 ± 0.1	0.57 ± 0.16
B	mg L ⁻¹	1 ± 0.02	0.99 ± 0.05	1.1 ± 0.04	1.22 ± 0.13	1.21 ± 0.07
Ba	mg L ⁻¹	0.84 ± 0.26	0.71 ± 0.36	0.46 ± 0.06	0.47 ± 0.1	0.53 ± 0.15
Ca	mg L ⁻¹	84 ± 3	94 ± 14	122 ± 18	143 ± 13	146 ± 20
DOC	mg L ⁻¹	n.d.	28.3 ± 19.34	6.77 ± 0.14	6.42 ± 0.35	17.02 ± 8.66
Fe	mg L ⁻¹	2.56 ± 0.79	2.96 ± 2.45	7.48 ± 2.35	18.3 ± 6.22	16.96 ± 14.91
FMeHg	ng L ⁻¹	0.44 ± 0.13	0.16 ± 0.01	0.37 ± 0.27	0.27 ± 0.09	0.89 ± 0.17
FTHg	ng L ⁻¹	259.85 ± 108.12	87.33 ± 18.03	251.98 ± 2.5	65.78 ± 35.19	168.25 ± 23.26
K	mg L ⁻¹	103.7 ± 15.99	105.1 ± 8.34	107.5 ± 7.78	138 ± 12.73	126 ± 14.14
Mg	mg L ⁻¹	164 ± 3	173 ± 16	197 ± 21	259 ± 1	249 ± 16
Mn	mg L ⁻¹	0.92 ± 0.05	1.03 ± 0.3	1.34 ± 0.21	2.16 ± 0.45	1.95 ± 0.95
Na	mg L ⁻¹	1457 ± 23	1450 ± 28	1545 ± 120	1895 ± 64	1875 ± 92
P	mg L ⁻¹	4.98 ± 0.12	4.28 ± 0.64	4.01 ± 0.4	3.16 ± 0.04	5.25 ± 1.34
pH		6.75 ± 0.01	6.78 ± 0.11	6.61 ± 0.06	6.42 ± 0.11	6.46 ± 0.26
S	mg L ⁻¹	58.03 ± 10.71	68.35 ± 15.63	112.15 ± 19.59	181 ± 4.24	154.5 ± 55.86
Si	mg L ⁻¹	14.6 ± 0.52	14.7 ± 0.57	15.2 ± 0.14	16.3 ± 0.57	16.8 ± 1.13
Sr	mg L ⁻¹	1.25 ± 0.03	1.37 ± 0.16	1.69 ± 0.23	2.03 ± 0.26	2.06 ± 0.32

sulfide	μM	0.28	0.45 ± 0.03	0.66 ± 0.15	0.65 ± 0.17	1.81 ± 0.32
Zn	mg L^{-1}	0.35 ± 0.01	0.27	0.35 ± 0.01	0.38 ± 0.02	0.32 ± 0.03
MeHg (solid)	ng gdw^{-1}	16.82	15.99 ± 1.3	16.34	15.35 ± 1.34	15.2 ± 0.17
THg (solid)	$\mu\text{g gdw}^{-1}$	46.24 ± 0.74	47.88 ± 2.43	47.91 ± 3.34	47.45 ± 0.81	47.61 ± 1.85

144 ^a The final two rows are solid-phase concentrations. Sediment was a silty mud collected to a depth of 15 cm from a tidal creek in the
 145 upper part of Berry's Creek in Bergen County, NJ. Sediment was amended with 5 wt% activated carbon (Calgon Type 3055, 80 x 325
 146 mesh, CAS #7440-44-0). Values represent averages \pm one s.d. (no s.d. denotes $n = 1$).



148 **Figure S7.** Correlation between passive sampler uptake and directly measured porewater
149 concentrations in sediment microcosm experiment across both amendment types and all time
150 points.

151

152 REFERENCES

- 153 Aoki D, Teramoto Y, Nishio Y. 2007. SH-containing cellulose acetate derivatives: preparation
154 and characterization as a shape memory-recovery material. *Biomacromolecules*
155 8(12):3749-3757.
- 156 Bernkop-Schnürch A, Kast CE, Richter MF. 2001. Improvement in the mucoadhesive properties
157 of alginate by the covalent attachment of cysteine. *J. Control. Release* 71(3):277-285.
- 158 Bhalekar M, Mangesh B, Savita S, Shamkant S. 2013. Synthesis and characterization of a
159 cysteine xyloglucan conjugate as mucoadhesive polymer. *Braz. J. Pharm. Sci.* 49(2):285-
160 292.
- 161 Charlionet R, Levasseur L, Malandin J-J. 1996. Eliciting macroporosity in polyacrylamide and
162 agarose gels with polyethylene glycol. *Electrophoresis* 17(58-66).
- 163 Choi J-H. 2010. Fabrication of a carbon electrode using activated carbon powder and application
164 to the capacitive deionization process. *Sep. Purif. Technol.* 70(3):362-366.
- 165 De Robertis A, Foti C, Patanè G, Sammartano S. 1998. Hydrolysis of (CH₃)Hg⁺ in different
166 ionic media: Salt effects and complex formation. *J. Chem. Eng. Data* 43(6):957-960.
- 167 Duan X, Lewis RS. 2002. Improved haemocompatibility of cysteine-modified polymers via
168 endogenous nitric oxide. *Biomaterials* 23(4):1197-1203.
- 169 Dyrssen D, Wedborg M. 1991. The sulphur-mercury(II) system in natural waters. *Water Air Soil
170 Pollut. Focus* 56(1):507-519.
- 171 Fernández-Gómez C, Bayona JM, Díez S. 2014. Comparison of different types of diffusive
172 gradient in thin film samplers for measurement of dissolved methylmercury in
173 freshwaters. *Talanta* 129:486-490.
- 174 Gao Y, de Canck E, Leermakers M, Baeyens W, van der Voort P. 2011. Synthesized
175 mercaptopropyl nanoporous resins in DGT probes for determining dissolved mercury
176 concentrations. *Talanta* 87:262-267.
- 177 Gao Y, De Craemer S, Baeyens W. 2014. A novel method for the determination of dissolved
178 methylmercury concentrations using diffusive gradients in thin films technique. *Talanta*
179 120:470-474.
- 180 Gomez-Eyles JL, Yupanqui C, Beckingham B, Riedel G, Gilmour C, Ghosh U. 2013. Evaluation
181 of biochars and activated carbons for in situ remediation of sediments impacted with
182 organics, mercury, and methylmercury. *Environ. Sci. Technol.* 47(23):13721-13729.
- 183 Graham AM, Cameron-Burr KT, Hajic HA, Lee C, Msekela D, Gilmour CC. 2017. Sulfurization
184 of dissolved organic matter increases Hg-sulfide-dissolved organic matter bioavailability
185 to a Hg-methylating bacterium. *Environ. Sci. Technol.* 51(16):9080-9088.
- 186 Ho YS, McKay G. 1998. Sorption of dye from aqueous solution by peat. *Chem. Eng. J.*
187 70(2):115-124.
- 188 Horvat M, Milena H, Lian L, Bloom NS. 1993. Comparison of distillation with other current
189 isolation methods for the determination of methyl mercury compounds in low level
190 environmental samples. *Anal. Chim. Acta* 282(1):153-168.
- 191 International Humic Substances Society (IHSS). 2018. Elemental Compositions and
192 Stable Isotopic Ratios of IHSS Samples. Denver (CO): IHSS. [cited 2019 February 1].
193 Available from: <http://humic-substances.org/elemental-compositions-and-stable-isotopic-ratios-of-ihss-samples/>
- 194 Karlsson T, Skyyberg U. 2003. Bonding of ppb levels of methyl mercury to reduced sulfur
195 groups in soil organic matter. *Environ. Sci. Technol.* 37(21):4912-4918.

- 197 Kast CE, Bernkop-Schnürch A. 2001. Thiolated polymers--thiomers: development and in vitro
198 evaluation of chitosan-thioglycolic acid conjugates. *Biomaterials* 22(17):2345-2352.
- 199 Lagergren S. 1898. Zur theorie der sogenannten adsorption gelöster stoffe. K. Sven.
200 Vetenskapsakad. Handl. 24(4):1-39.
- 201 Liem-Nguyen V, Skjellberg U, Björn E. 2016. Thermodynamic modeling of the solubility and
202 chemical speciation of mercury and methylmercury driven by organic thiols and
203 micromolar sulfide concentrations in boreal wetland soils. *Environ. Sci. Technol.*
204 51(7):3678-3686.
- 205 Loux NT. 2007. An assessment of thermodynamic reaction constants for simulating aqueous
206 environmental monomethylmercury speciation. *Chem. Spec. Bioavail.* 19(4):193-206.
- 207 Manceau A, Nagy KL. 2012. Quantitative analysis of sulfur functional groups in natural organic
208 matter by XANES spectroscopy. *Geochim. Cosmochim. Acta* 99:206-223.
- 209 Mitchell CPJ, Gilmour CC. 2008. Methylmercury production in a Chesapeake Bay salt marsh. *J.
210 Geophys. Res.* 113(G2):G00C04.
- 211 Qian J, Jin Q, Ulf S, Wolfgang F, Bleam WF, Bloom PR, Petit PE. 2002. Bonding of methyl
212 mercury to reduced sulfur groups in soil and stream organic matter as determined by x-
213 ray absorption spectroscopy and binding affinity studies. *Geochim. Cosmochim. Acta*
214 66(22):3873-3885.
- 215 Rabenstein DL, Tourangeau MC, Evans CA. 1976. Proton magnetic resonance and Raman
216 spectroscopic studies of methylmercury(II) complexes of inorganic anions. *Can. J.
217 Chem.* 54(16):2517-2525.
- 218 Reid RS, Rabenstein DL. 1981. Nuclear magnetic resonance studies of the solution chemistry of
219 metal complexes. XVII. Formation constants for the complexation of methylmercury by
220 sulphydryl- containing amino acids and related molecules. *Can. J. Chem.* 59:1505.
- 221 Schwarzenbach G, Schellenberg M. 1965. Die komplexchemie des methylquecksilber-kations.
222 *Helv. Chim. Acta* 48(1):28-46.
- 223 Spectrum Brands. 2008. Instant Ocean SeaScope Volume 24. Madison (WI): Spectrum Brands.
224 [cited 2019 February 1]. Available from:
225 http://www.instantocean.com/~media/UPG/Files/Instant%20Ocean/SeaScope/Volume%2024_Fall_2008.ash
- 226 Sukitpaneenit P, Chung T-S. 2009. Molecular elucidation of morphology and mechanical
227 properties of PVDF hollow fiber membranes from aspects of phase inversion,
228 crystallization and rheology. *J. Memb. Sci.* 340(1-2):192-205.
- 229 Tien C, Ramarao BV. 2017. On the significance and utility of the Lagergren model and the
230 pseudo second-order model of batch adsorption. *Separ. Sci. Technol.* 52(6):975-986.
- 231 Yu Y, Addai-Mensah J, Losic D. 2012. Functionalized diatom silica microparticles for removal
232 of mercury ions. *Sci. Technol. Adv. Mater.* 13(1):1-11.
- 233
- 234